Published in final edited form as:

Arterioscler Thromb Vasc Biol. 2018 June ; 38(6): 1271–1282. doi:10.1161/ATVBAHA.117.310082.

Protease-activated Receptor 2 Deficiency Attenuates Atherosclerosis in Mice

Shannon M. Jones, B.S.[1], **Adrien Mann, B.S.**[1], **Kelsey Conrad, M.S.**[1,2], **Keith Saum, B.S.**[1,3], **David E. Hall, M.S.**[4], **Lisa M. McKinney, B.S.**[1], **Nathan Robbins, M.S.**[1], **Joel Thompson, Ph.D.**[5], **Abigail D. Peairs, Ph.D.**[4], **Eric Camerer, Ph.D.**[6], **Katey J. Rayner, Ph.D.**[7], **Michael Tranter, Ph.D.**[1,2], **Nigel Mackman, Ph.D.**[8], and **A. Phillip Owens III, Ph.D.**[1,2]

[1]Division of Cardiovascular Health and Disease, Department of Internal Medicine, The University of Cincinnati College of Medicine, Cincinnati, OH, 45267-0542, USA, Phone: 513-558-3428

[2]Pathobiology and Molecular Medicine Program, Department of Internal Medicine, The University of Cincinnati College of Medicine, Cincinnati, OH, 45267-0542, USA, Phone: 513-558-3428

[3]University of Cincinnati Medical Scientist Training Program, Department of Internal Medicine, The University of Cincinnati College of Medicine, Cincinnati, OH, 45267-0542, USA, Phone: 513-558-3428

[4]Department of Nutritional Sciences, College of Allied Health, Department of Internal Medicine, The University of Cincinnati College of Medicine, Cincinnati, OH, 45267-0542, USA, Phone: 513-558-3428

[5]Division of Endocrinology and Molecular Medicine, Department of Internal Medicine, The University of Kentucky, Lexington, KY, 40536-0200, USA, Phone: 859-323-5821

[6]INSERM U970, Paris Cardiovascular Research Centre, 56 Rue Leblanc, Paris, France F-75015, Phone: +33 (0)1 53 98 80 48

[7]Department of Biochemistry, Microbiology, and Immunology, University of Ottawa Heart Institute, Ottawa, Ontario, Canada K1H 8M5, Phone: 613-761-5283

[8]Division of Hematology and Oncology, Department of Medicine, UNC McAllister Heart Institute, University of North Carolina at Chapel Hill, Chapel Hill, NC 27599, USA, Phone: 919-843-3961

Abstract

Objective—Protease-activated receptor 2 (PAR2)-dependent signaling results in augmented inflammation and has been implicated in the pathogenesis of several autoimmune conditions. The objective of this study was to determine the effect of PAR2 deficiency on the development of atherosclerosis.

Approach and Results—PAR2 mRNA and protein expression is increased in human carotid artery and mouse aortic arch atheroma versus control carotid and aortic arch arteries, respectively.

Address for Correspondence: A. Phillip Owens III, Ph.D., University of Cincinnati, 231 Albert Sabin Way ML: 0542, Cincinnati, OH 45267-0542, Telephone: (513) 558 3428, Fax: (513) 558 4545, phillip.owens@uc.edu.

Disclosures

None

To determine the effect of PAR2 deficiency on atherosclerosis, male and female low density lipoprotein receptor deficient ($Ldlr^{-/-}$) mice (8–12 weeks old) that were $Par2^{+/+}$ or $Par2^{-/-}$ were fed a fat and cholesterol-enriched diet for 12 or 24 weeks. PAR2 deficiency attenuated atherosclerosis in the aortic sinus and aortic root after 12 and 24 weeks. PAR2 deficiency did not alter total plasma cholesterol concentrations or lipoprotein distributions. Bone marrow transplantation showed that PAR2 on non-hematopoietic cells contributed to atherosclerosis. PAR2 deficiency significantly attenuated levels of the chemokines *Ccl2* and *Cxcl1* in the circulation and macrophage content in atherosclerotic lesions. Mechanistic studies using isolated primary vascular smooth muscle cells showed that PAR2 deficiency is associated with reduced *Ccl2* and *Cxcl1* mRNA expression and protein release into the supernatant resulting in less monocyte migration.

Conclusions—Our results indicate PAR2 deficiency is associated with attenuation of atherosclerosis and may reduce lesion progression by blunting *Ccl2* and *Cxcl1* induced monocyte infiltration.

Keywords

Atherosclerosis; protease-activated receptor 2; vascular smooth muscle cells

Introduction

Atherosclerosis is a chronic and progressive inflammatory disease defined as stenosing of blood vessels, which may lead to rupture or erosion of unstable plaques, resulting in acute atherothrombotic occlusion of blood flow to the brain (ischemic stroke) or heart (myocardial infarction – MI).[1] The disease is characterized by infiltration of lipids, platelets, neutrophils, monocyte/macrophages (foam cells), T and B lymphocytes, and replication and migration of vascular smooth muscle cells (VSMCs) into the vessel walls of large arteries. This infiltration of immune cells results in local release of several classes of proteases implicated in all stages of atherosclerotic disease, including: intimal thickening, plaque progression, and plaque rupture. Comprising a third of the protease compliment in an entire organism (degradome), serine proteases are crucial activators of the coagulation cascade and can activate cells through membrane bound protease-activated receptors (PARs).[2]

The four members of the PAR family (PAR1 – 4) are ubiquitously expressed by vascular cells and are activated via proteolytic cleavage of their N-terminal domain, exposing a tethered ligand.[3] PAR1, 3, and 4 are preferentially cleaved by the serine protease thrombin, an essential enzyme in hemostasis and thrombosis.[4] Studies utilizing direct thrombin inhibitors (DTIs) or prothrombotic mice have shown that thrombin contributes to the initiation of atherosclerosis in murine models.[5–7] However, one study found that PAR4 deletion in mice has no effect on atherosclerosis.[8] Recent investigations have suggested that PAR1 may be the primary thrombin receptor for the initiation of atherosclerosis. Thrombin activation of PAR1 promotes the migration and proliferation of VSMCs, cytokine and chemokine expression, vascular calcification, and cellular apoptosis.[9–12] In addition, the binding of thrombin to PAR1 can result in transactivation of PAR2.[13, 14] PAR1 is also present and upregulated in both mouse and human atherosclerotic lesions.[15, 16] Further analysis is required to better understand the role of thrombin activation of PARs in the development of atherosclerosis.

PAR2 is activated by the serine proteases trypsin, tryptase, and the tissue factor (TF)/factor VIIa (FVIIa) complex or FXa, but not by thrombin. PAR2 expression is increased in the atherosclerotic aorta of apolipoprotein E deficient ($apoE^{-/-}$) mice compared to normolipidemic controls.[15–17] In addition, it is upregulated in atherosclerotic human coronary arteries and is localized to intimal VSMCs.[15–17] PAR2 activation in coronary artery VSMCs results in the secretion of multiple pro-atherogenic cytokines and chemokines, including IL-6, IL-8, and CCL2.[18] PAR2 deficiency is associated with reduced intimal VSMC hyperplasia in acarotid artery ligation model.[14] VSMC hyperplasia in this model results from VSMC de-differentiation and proliferation, which is a common phenotype in early and late stage atherosclerotic lesion formation and progression, respectively.[19–21]

In this study, we investigated the role of PAR1 and PAR2 in diet-induced atherosclerosis utilizing the low-density lipoprotein receptor deficient ($Ldlr^{-/-}$) mouse model in conjunction with total PAR1 and PAR2 deficiency. Utilizing bone marrow transplantation, we determined the relative contribution of hematopoietic or non-hematopoietic PAR2 in atherosclerotic disease. Finally, we examined the effects of PAR2 deficiency on atherosclerotic inflammation in mice and extended these findings to cell culture studies with primary murine VSMC.

Materials and Methods

Mice and diet

Original $Par1^{-/-}$ and $Par2^{-/-}$ mice were obtained from R.W. Johnson Pharmaceutical Research Institute and were 11 and 6 times backcrossed into C57BL/6J, respectively.[22, 23]

$Ldlr^{-/-}$ mice (B6.129S7-$Ldlr^{tm1Her}$, stock no. 002207, N12) were obtained from The Jackson Laboratory (Bar Harbor, MA). $Ldlr^{-/-}/Par1^{+/+}$ and $Ldlr^{-/-}/Par1^{-/-}$ cousin littermate mice (final N12) were generated by interbreeding $Ldlr^{-/-}/Par1^{+/-}$ mice, which were created by breeding $Ldlr^{-/-}/Par1^{-/-}$ onto the Jackson $Ldlr^{-/-}$ strain. A similar strategy was used to generate $Ldlr^{-/-}/Par2^{+/+}$ and $Ldlr^{-/-}/Par2^{-/-}$ littermates (final N8). Our original study with PAR2 deficient animals utilized both male and female mice (8 – 10 weeks of age). As there was no significant difference between the two sexes, we utilized male mice (8 – 10 weeks of age) for the remainder of our studies.

All mice were fed a normal mouse laboratory diet and water ad libitum. To induce hypercholesterolemia in the majority of studies, mice were fed a diet enriched with saturated milk fat (21% wt/wt) and cholesterol (0.15% wt/wt, diet TD.88137 from Harlan Teklad, produced by Purina Lab Diets, Land O' Lakes Inc.). For the semisynthetic diet, we utilized a low-fat (4.3% fat wt/wt) modified AIN76A diet containing 0.15% cholesterol, as described by Teupser and colleagues (Purina Lab Diets, Land O' Lakes Inc.).[24]

Bone marrow transplantation

Mice were given sulfamethoxazole and trimethoprim oral suspension (0.2%; Hi Tech Pharmacal Co.) in their water, ad libitum, for 1 week prior to and 5 weeks after irradiation. Male recipient $Ldlr^{-/-}/Par2^{+/+}$ and $Ldlr^{-/-}/Par2^{-/-}$ mice (8 weeks old) were irradiated with a

total of 13 Gy (2 doses of 650 rads 4 hours apart) using a Cs^{137} irradiator (JL Shepherd, San Fernando, CA). Irradiated mice were re-populated with bone marrow harvested from *Ldlr*$^{-/-}$/*Par2*$^{+/+}$ and *Ldlr*$^{-/-}$/*Par2*$^{-/-}$ mice donor mice via retro-orbitally injected cells (1 x 10^7 cells per mouse). Mice were allowed to recover for 5 weeks and then fed a 'Western' diet for 12 weeks.

Plasma collection and processing of heart and aorta

Mice were sedated with 3% isoflurane and blood was collected from the inferior vena cava into a 25 gauge x 1′ needle pre-coated with 3.8% sodium citrate. The mice were then humanely euthanized. An aliquot of blood was analyzed for complete blood count utilizing a Hemavet 950 LV veterinary multi-species hematology system (Drew Scientific). Blood was centrifuged at 4,000 x g for 15 minutes to prepare platelet poor plasma and then stored at −80°C until use. The heart, aorta, and body were perfused with sterile saline injected into the left ventricle at physiologic pressure. Hearts were separated from the aorta under a dissecting microscope and then placed in optimal cutting temperature (OCT), frozen, and stored at −80°C until processed. The majority of aortas were extracted and placed into formalin (10% wt/vol) for 48 hour fixation, before being switched to sterile saline and then stored until dissection and processing. Several aortic arches were processed, after diet, for mRNA and protein (described in later sections).

Plasma lipid analyses

Mouse plasma lipid concentrations were analyzed with the following commercially kits: total plasma cholesterol (Total Cholesterol E), triglycerides (L-Type TG M), LDL-C (L-Type LDL-C), and HDL-C (L-Type HDL-C) from Wako Chemicals (Richmond, VA).

Aortic sinus atherosclerosis quantification

Atherosclerotic lesions in the aortic sinus were cut and processed as previously described.[25] Briefly, hearts were thawed from −80°C storage in OCT, and cut parallel to the tricuspid valve approximately 3mm from the base of the ventricles. The aortic sinus was placed perpendicular to the bottom of a tissue mold and then covered in OCT and sectioned. After the appearance of the full tricuspid valve leaflets, the aortic sinus was serially sectioned in 10μm increments over the course of at least 8 – 10 microscope slides with at least 9 sections/slide covering a distance of ~720μm from the aortic sinus extending into the ascending aorta. Slides were then stained with Oil-red-O, counterstained with hematoxylin/eosin, mounted, and lesion area quantified utilizing NIH Image J Fiji software (NIH, Bethesda, MD). All quantification was verified by at least two blinded observers.

En face atherosclerosis quantification

En face atherosclerosis was performed and quantified, as previously described. Briefly, aortas were removed from storage in sterile saline and cleaned free of all adventitia. The left subclavian artery was removed, and all but 1mm of the innominate/brachiocephalic and left common carotid artery was removed for standardization purposes. The aorta was then cut open along the outer curvature along the innominate and left common carotid artery down to the subclavian artery. The inner curvature was then cut open from the ascending aorta down

to the iliac bifurcation. The aorta was pinned flat with dissection pins onto a tray fitted with sudan black stained paraffin. Aortic arch was defined as the beginning of the ascending aortic arch to 3mm distal the subclavian artery. Thoracic aorta was 3mm distal the subclavian artery to the last intercostal artery. Abdominal aorta was defined as last intercostal artery to the iliac bifurcation. Images were taken with a Nikon SMZ800N dissecting microscope with 16MP camera. All images were taken in range of a ruler with standard millimeter hash marks at the same depth and magnification. Atherosclerotic lesions were quantified by percentage of atherosclerotic area versus the total area of the aorta being addressed using Image J Fiji software (NIH, Bethesda, MD). All atherosclerotic quantification was verified by at least two blinded users.

Immunohistochemistry and histologic processing of aortic sinuses

Histological analysis was performed on fresh frozen aortic sinus sections utilizing Picrosirius Red (PolyScientific, cat# 24901-500). Images were captured utilizing a polarizing microscope with 10x objective (Nikon Optiphot Polarizing Microscope). Immunostaining was performed on frozen serial sections as described previously.[26] Human carotid atherosclerotic sections were obtained from Origene Technologies, Inc. Briefly, sections were fixed with ice cold ethanol, and stained with SMC α-actin 1A4 Cy3 conjugated antibody (5 μg/ml; Sigma Aldrich, cat #C6198). Human and mouse PAR2 staining was performed with mouse monoclonal anti-PAR2 Alexa Fluor 488 (1/50 dilution; SAM11; SC-13504 AF488; Santa Cruz Biotechnologies). Sections were mounted with prolong gold anti-fade mounting solution (Thermo Fisher) and images visualized on a fluorescent microscope (Olympus 1X71). Immunostaining of CD68 utilized a rat anti-CD68 antibody (FA-11; Catalog number MCA1957, AbD Serotec; 1/50 dilution incubated overnight 4ºC). Subsequent application of a goat anti-rat (mouse absorbed) biotinylated antibody (Vector, BA-9401; 1/500 dilution incubated 1 hour room temperature). Positive reactive areas were visualized via application of an ABC kit (15 minutes 37ºC) and subsequent detection with AEC chromogen (2 applications of 10 minutes room temperature; Vector). Several controls were used, including: no primary antibody, no primary and secondary antibodies, and non-immune IgG (not shown). Images were captured with a 4x, 10x, and 20x objective lens using a Nikon Eclipse FN1 scope.

Mouse aortic VSMC isolation

Mouse aortic arch VSMCs were isolated as previously described with several modifications.[27] Briefly, we only utilized the heavily atherosclerotic prone region of the aortic arch, extending from the start of the ascending aorta to 3 mm distal the subclavian artery (including the innominate and left common carotid arteries) for purposes of standardization. Aortic arches and associated vessels were removed from $Par2^{+/+}$ and $^{-/-}$ mice (aged 6 – 7 weeks) and dissected free of all adventitia in sterile saline solution. Aortas were then allowed to incubate in a solution of 1 mg/mL collagenase type II (Worthington Chemical) for 15 minutes at 37ºC with 5% CO_2. Aortas were then taken, dissected open, and endothelium removed with a sterile Q-tip. Aortas were cut into small pieces and placed in a solution of 1 mg/mL collagenase type II (Worthington Biochemical, catalog LS004174), 1 mg/mL soybean trypsin inhibitor (Worthington Biochemical LS003570), elastase (Worthington Biochemical LS002279, final concentration ~1 U/mL), and 1% penicillin/

streptomycin (Gibco) made in sterile 1x phosphate buffered saline (PBS) for 1 hour, as previously described.[28] After 1 hour of incubation, aortas were triturated with a 21 gauge needle repeatedly until tissues were broken apart. VSMCs were then maintained in DMEM with fetal bovine serum (20% vol/vol: FBS, Omega Scientific) and penicillin/streptomycin (1% wt/vol, Gibco) in a cell culture incubator. VSMC phenotype was verified via staining and visualization of SMC α-actin clone 1A4 Cy3 labeled (Sigma Aldrich).

Quantitative real-time polymerase chain reaction (qRT-PCR)

Total ribonucleic acid (RNA) was isolated from the aortic arches of *Ldlr*$^{-/-}$ mice fed a normal chow or 'Western' diet for 24 weeks as previously described (n = 15 each group, 3 aortas combined into one sample for 5 individual samples) and described below.[27] RNA was also isolated from VSMCs using the TRIzol® method (Invitrogen, catalog #18091200) and reverse transcribed into complimentary deoxyribonucleic acid (cDNA) using random hexamers in a SuperScript™ IV first-strand synthesis system kit (Invitrogen, Carlsbad, CA). Levels of different messanger RNAs (mRNAs) were analyzed by real-time PCR using TaqMan™ Fast Advanced Master Mix and Stratagene Mx3005P (Agilent Technologies). We utilized TaqMan probe sets with the following catalog numbers: Human *PAR1* (Hs00608346_m1), Mouse *Par1* (Mm00433160_m1), Human *PAR2* (Hs00608346_m1), Mouse *Par2* (Mm00433160_m1), Mouse Ccl2 (Mm00441243_g1), and Mouse Cxcl1 (Mm04207460_m1). All human mRNA was extrapolated to 18s rRNA (Hs99999901_s1) and mouse mRNA was extrapolated to Hprt (Mm00446968_m1).

Human carotid artery atherosclerotic samples

Human carotid artery atherosclerotic samples were obtained from Origene Technologies, Inc. Briefly, frozen sections (n = 5 patient samples, 25 sections per patient) were purchased and protein (20 combined sections/patient) and mRNA (5 combined sections/patient) were obtained utilizing a previously established method by Vrana and colleagues and an RNAqueous™-Micro total RNA isolation kit (Thermo Fisher/Ambion; catalog #AM1931), respectively.[29]

Boyden Chamber Assay

Monocyte migration and chemotaxis was measured with a 5 μm pore size chemotaxis assay in a 96 well plate (Cell Biolabs Inc., catalog # CBA-105) per company specifications. Briefly, *Par2*$^{+/+}$ and $^{-/-}$ aortic arch VSMCs were isolated, as described above, and plated in a 96 well plate at a density of 1.0 x 10^3 cells/well. After one week of growth, cells were serum starved for 24 hours and treated with control LDL (50 μg/mL, Alfa Aesar Catalog # BT-903), recombinant mouse IL-1β (10 ng/mL; catalog 401-ML/CF; R & D Systems, Inc.), recombinant mouse TNFα (100 ng/mL; catalog 410-MT/CF; R & D Systems, Inc.), or oxidized LDL (oxLDL, 50 μg/mL, Alfa Aesar Catalog # BT-910) for 24 hours. Media was then harvested, centrifuged, and supernatant collected. Media was directly added to another 96 well plate with migration membranes and THP-1 monocytes (ATCC) were added to the top chamber. After 24 hours of incubation, monocyte migration through the membrane was detected via fluorescent staining, as per company instructions.

PAR2 ELISA

PAR2 protein in both mouse and human samples were measured utilizing a sandwich ELISA. Polyclonal rabbit anti-human PAR2 (PA5-33527, Invitrogen) was coated onto Nunc MaxiSorp flat-bottom 96 well plates (2 μg/mL antibody in 50 μl) overnight at 4ºC. Wells were then washed 3x and 200 μl/well with 1x PBS/0.1% Triton X-100, and then blocked with 200 μl 3% BSA and 0.1% Triton X-100 in 1x PBS for 2 hours in a humidity chamber. Wells were then washed 3x and 200 μl/well with 1x PBS/0.1% Triton X-100. Utilizing normal and atherosclerotic aortic arches (mice) and normal and atherosclerotic carotid arteries (human) we added 1 μg of protein diluted in 50 μl of 0.2% BSA/0.1% Triton X-100/1 μl protease inhibitor cocktail (Sigma P4830) to each well for 1 hour at 37ºC in triplicate. PAR2 recombinant protein (Abcam; catalog #ab152372) ranging from 1 μg/mL to 15.5 ng/mL serially diluted was used as a calibration curve. Wells were then washed 3x and 200 μl/well with 1x PBS/0.1% Triton X-100. HRP-conjugated monoclonal mouse anti-human PAR2 (SAM-11, Santa Cruz, catalog #sc-13504 HRP) was added to each well (1:1000 dilution in 1x PBS/0.2% BSA/0.1% Triton X-100, 50 μl/well) and incubated for 1 hour at 37ºC. Wells were washed 3x with 200 μl/well of 1x PBS/0.1% Triton X-100 and then 50 μl of substrate solution (TMB Super Sensitive 1 Component HRP MIcrowell substrate (SUBS); Biomol, catalog #ICT-6329) for 30 minutes at room temperature. The reaction was then halted using 100 μl stop solution for TMB microwell substrate (STOPT, Biomol, catalog #ICT-6343). Absorbance was read within 10 minutes at 450 nm using a Cytation 3 (Bio-Tek). Absorbance values of the standards were extrapolated to a non-linear third degree polynomial equation. Protein from PAR2 deficient aortas and VSMC cultures was not detected utilizing this ELISA (data not shown). While a previous publication demonstrated that SAM11 was not specific for PAR2 in arterial lysates of PAR2 deficient mice, our studies utilize a polyclonal capture of PAR2 before detection with the SAM11 antibody; which confers specificity in an ELISA setting.[30]

Commercial ELISAs

The following commercially available kits were used for determining protein and supernatant concentrations of MCP-1 and CXCL1: MCP-1 mouse quantikine kit (R&D Systems, Inc.; catalog #MJE00) and CXCL1/KC/Gro mouse quantikine kit (R&D Systems, Inc.; catalog #MKC00B).

Protein assay

Where applicable, protein was quantified in cell or tissue samples utilizing the DC protein assay (BioRad Inc.) in the 96 well plate assay according to the product manual.

Research statistics and data representation

All bar and line graphs were created with Sigma Plot v.13 (SPSS, Chicago, IL). All statistical analysis was performed using SigmaStat, now incorporated into Sigma Plot v.13. Data are represented as mean ± SEM. For two group comparison of parametric data, a Student’s t-test was performed, while non-parametric data was analyzed with a Mann-Whitney Rank Sum. Statistical significance between multiple groups was assessed by One Way analysis of variance (ANOVA) on Ranks with a Dunn’s post hoc, One Way ANOVA

with Holm Sidak Post Hoc, or Two Way ANOVA with Holm Sidak Post Hoc, when appropriate. Statistical significance among groups performed temporally was assessed by either a One Way Repeated Measures ANOVA (parametric) or Repeated Measures ANOVA on Ranks (non-parametric), where appropriate. Values of $P < 0.05$ were considered statistically significant.

Study approvals

All mouse studies were performed with the approval of the UNC-CH and the University of Cincinnati Institutional Animal Care and Use Committees.

Results

PAR1 and PAR2 expression is increased in mouse and human atherosclerotic prone regions

PAR2 expression was measured in normal and atherosclerotic specimens from both mice and humans. Male low density lipoprotein deficient ($Ldlr^{-/-}$) mice were fed either a control or high fat and cholesterol 'Western' diet for 24 weeks and aortic arches were harvested. We also used human atherosclerotic carotid artery specimens and age-matched healthy human control arteries. We found that *Par2* mRNA and protein were significantly elevated in atherosclerotic versus normal vessels in both mouse and human arterial tissue (Figure 1A–D). Importantly, this increased expression is similar in mouse and human atherosclerotic arteries (mRNA: 32 vs 42 fold; protein: 7.0 vs 9.5 fold respectively). PAR2 protein expression was further assessed in the atherosclerotic aortic sinus (mice) and carotid artery (human) by immunofluorescence (Figure 1E – 1J, negative controls Supplemental Figure I). The majority of PAR2 protein expression is localized to the tunica media containing VSMCs compared to the atherosclerotic lesion (Figure 1G and 1J) in both species.

Similar to PAR2, *Par1* mRNA (Supplemental Figure IIA – IIB) was significantly elevated in the atherosclerotic versus normal vessels in both mouse and human arterial tissue. PAR2 deficiency had no effect on atherosclerotic-induced Par1 mRNA regulation in $Ldlr^{-/-}$ mice fed a Western diet for 12 or 24 weeks (Supplemental Figure IIIC).

Effect of PAR1 or PAR2 deficiency is associated with reduced diet-induced atherosclerosis in mice

To examine the contribution of PAR2 in atherosclerosis, we examined 8 – 10 week old male and female $Ldlr^{-/-}/Par2^{+/+}$ and $Ldlr^{-/-}/Par2^{-/-}$ mice (n = minimal 16 each group) fed a Western diet for 12 weeks. Compared to proficient controls, PAR2 deficiency was associated with dramatically less atherosclerosis in both the aortic sinus and aortic arch independent of gender (Figure 2A – 2F). Histological examination of the aortic sinus showed significantly less macrophage accumulation (Figure 2G, 71% decrease), an increase in VSMC α-actin (Figure 2H, 152% increase), and an increase in Type I collagen (Figure 2I, 490% increase) in PAR2 deficient mice compared to controls.

PAR2 deficiency did not affect total plasma cholesterol concentrations or individual lipoproteins (Table 1). However, we did observe decreased weight gain, liver weight, and fat

pad weights in PAR2 deficient mice versus normal controls (Supplemental Figure III). This observation is consistent with a previous study demonstrating a role for PAR2 in diet-induced obesity.[31] To eliminate an effect of changes in weight gain on atherosclerosis, we utilized a low-fat (4.3% fat wt/wt) modified AIN76A semisynthetic diet containing 0.15% cholesterol (high cholesterol diet; HCD) in a cohort of male *Ldlr*$^{-/-}$/*Par2*$^{+/+}$ and *Ldlr*$^{-/-}$/*Par2*$^{-/-}$ mice (n = 9 each genotype) for 12 weeks. Similar increases in cholesterol to the 'Western' diet were observed with this diet without the complications of PAR2-dependent changes in weight gain, hyperglycemia, insulin resistance, or hypertension.[24] The mice fed the HCD gained minimal weight (not significantly different between the genotypes) and similar to Figure 2, PAR2 deficiency was associated with less atherosclerosis (Supplemental Figure IV).

To determine if PAR1 influences atherosclerosis, *Ldlr*$^{-/-}$/*Par1*$^{+/+}$ and *Ldlr*$^{-/-}$/*Par1*$^{-/-}$ mice (n = 9 each group) were fed a Western diet for 12 weeks. Atherosclerosis was quantified in the aortic sinus and aortic root of these mice. We found that PAR1 deficiency had no effect on diet-induced atherosclerosis compared to proficient controls (Supplemental Figure VA – VB and VD – VE). Further, there was no difference in macrophage accumulation suggesting no differences in infiltration or cellularity (Supplemental Figure VC and VF – VG). No differences were observed between genotypes regarding total plasma cholesterol, lipoprotein distribution, or weight. These results indicate that PAR1 does not play a role in the development of atherosclerosis in the *Ldlr*$^{-/-}$ model of atherosclerosis.

PAR2 on non-hematopoietic cells contributes to atherosclerosis

We utilized bone marrow transplantation to define the cellular source of PAR2 that contributes atherosclerosis. Irradiated male *Ldlr*$^{-/-}$/*Par2*$^{+/+}$ (n = 11 – 13) and *Ldlr*$^{-/-}$/*Par2*$^{-/-}$ (n = 9 – 10) mice were transplanted with bone marrow from either *Ldlr*$^{-/-}$/*Par2*$^{+/+}$ or *Ldlr*$^{-/-}$/*Par2*$^{-/-}$ mice. Transplanted mice were given a 5 week rest period, and then fed a 'Western' diet for 12 weeks. Atherosclerosis in the aortic sinus and aortic arch was significantly less in all *Ldlr*$^{-/-}$/*Par2*$^{-/-}$ mice independent of recipient genotype (Figure 3A – 3C). All groups with PAR2 deficiency (both hematopoietic and non-hematopoietic) gained significantly less weight than the PAR2 proficient control group (Table 1, Supplemental Figure VI). This weight difference did not affect the outcome of the atherosclerosis studies, as demonstrated by hematopoietic deficiency of PAR2 having similar weight to non-hematopoietic PAR2 deficient mice with a greatly increased burden of atherosclerosis. Deficiency of PAR2 in the non-hematopoietic lineage recapitulated the content of the aortic sinus observed in mice with a global deficiency in PAR2 with less macrophage accumulation (Figure 3D, 79% decrease), an increase in medial SMC α-actin (Figure 3E, 222% increase), and an increase in Type I collagen (Figure 3F, 443% increase) when compared to PAR2 deficiency in the hematopoietic compartment and control mice.

PAR2 deficiency results in a protective plaque phenotype

To determine the role of PAR2 in a chronic progression model, we examined male *Ldlr*$^{-/-}$/*Par2*$^{+/+}$ and *Ldlr*$^{-/-}$/*Par2*$^{-/-}$ mice (8 – 10 weeks of age, n = 12 mice per genotype) fed a 'Western' diet for 24 weeks. PAR2 deficiency was associated with significantly less atherosclerotic burden in the aortic sinus and aortic root compared to proficient controls in

an advanced model of atherosclerosis (Figure 4A – B). PAR2 deficiency was associated with more robust VSMC α-actin expression as a percentage of the total lesion (Figure 4D and 4E, 4G and 4H – 255% increase; $P < 0.001$) and a thicker fibrous cap (Figure 4G, 4I, and 4J – 105% increase; $P < 0.001$). PAR2 deficiency also resulted in less necrotic core area as measured by acellular regions (Figure 4C, 4F, and 4H # in picture). Finally, PAR2 deficiency attenuated secondary lesion formation on top of the fibrous cap (represented by * in Figure 4C) quantified as macrophage positive area (data not shown; +/+: 15 ± 4.2%; −/−: 3.2 ± 1.1%; $P < 0.001$). No differences in total plasma cholesterol, triglycerides, or lipoprotein distribution were found between the different genotypes (Table 1). Similar to the acute experiments in Figure 2, PAR2 deficiency significantly reduced weight gain during chronic feeding (Table 1, Supplemental Figure VI). However, no significant difference was observed in weight at the penultimate 23 and 24 week time points demonstrating a 'catch-up' effect at the end of the study.

PAR2 deficiency attenuates the production of chemokines

Previous studies have shown PAR2 has a critical role in the production of pro-inflammatory cytokines and chemokines in vitro and in vivo.[14, 15] Therefore, we examined the level of several atherosclerotic pro-inflammatory cytokines and chemokines in the plasma from our acute and chronic studies. While several cytokines were lower in PAR2 deficient mice, the chemokines CCL2 (also known as monocyte chemoattractant protein 1MCP-1; ~80% less) and CXCL1 (also called KC or N51; ~75% less) were significantly attenuated in PAR2 deficient mice versus normal controls at both 12 and 24 week time points (Figure 5A). These chemokines were also decreased in all PAR2 deficient recipients upon analysis of the bone marrow transplantation experiments (Figure 5B). We also measured chemokine mRNA and protein isolated from the aortic arch (n = 5 each genotype/time point) of 8 – 10 week old male *Ldlr*$^{-/-}$/*Par2*$^{+/+}$ and *Ldlr*$^{-/-}$/*Par2*$^{-/-}$ mice were fed a 12 or 24 week 'Western' diet, We found that PAR2 deficiency was associated with significantly less expression of *Ccl2* and *Cxcl1* mRNA (Figure 5C) and protein (Figure 5D – 5E) in the aortic arch of atherosclerotic mice.

PAR2 mediates smooth muscle cell-induced cytokine expression and monocyte chemotaxis

VSMCs play a critical role in atherogenesis via phenotypic modulation to a synthetic state characterized by increased proliferation, migration, and loss of contractile proteins, such as α-actin.[32] Our data demonstrates PAR2 deficiency attenuates the loss of α-actin expression in early lesions. In addition, PAR2 is a potent mediator of VSMC mitogenesis via the activation of NF-κB and ERK1/2.[15, 33–37] Activation of PAR2 also increased expression of key proinflammatory cytokines IL-1β and TNFα,[38, 39] which are critical mediators of CCL2.[40–42] Together with our non-hematopoietic chimeras, we examined the contribution of VSMC PAR2 to of CCL2 and CXCL1 expression. To assess if PAR2 deficient VSMCs have an effect on CCL2 or CXCL1 expression, we evaluated the response of *Par2*$^{+/+}$ and *Par2*$^{-/-}$ VSMCs to the pro-inflammatory cytokines to IL-1β (10 ng/mL), TNFα (100 ng/mL), and the atherogenic ligand oxidized LDL (oxLDL, 50 μg/mL) compared to PAR2 agonist peptide (AP, SLIGRL-NH2, 100μM) and the placebo control LDL. *Ccl2 and Cxcl1* mRNA expression in VSMCs and secreted *Ccl2 and Cxcl1* were significantly attenuated in PAR2

deficient cells under all treatment conditions (Figure 6A – 6D). Interestingly, basal levels of *Ccl2* were significantly decreased in *Par2*$^{-/-}$ VSMCs compared to *Par2*$^{+/+}$ (Supplemental Figure VII; no change in *Cxcl1*). Finally, monocyte migration was attenuated in a Boyden chamber with *Par2*$^{-/-}$ VSMCs treated with IL-1β, TNFα, or oxLDL (Figure 6G) compared to *Par2*$^{+/+}$ controls. Pretreatment with a CCL2/CXCL1 antibody cocktail significantly decreased IL-1β, TNFα, and oxLDL-induced monocyte migration (data not shown; $P < 0.001$ all versus all agonists).

Discussion

We confirmed the presence of PAR1 and PAR2 in both mouse and human atherosclerotic lesions. Importantly, we found that PAR2 deficiency but not PAR1 deficiency is associated with decreased early and late stage atherosclerosis. In the PAR2 deficient mice we observed less macrophage accumulation, more medial SMC α-actin expression, and reduced type I collagen deposition in acute and chronic atherosclerosis. Similar results were observed when PAR2 was deleted in non-hematopoietic cells. This effect was not dependent upon changes in cholesterol and lipid profiles, or its effects on body weight. After the completion of our study, another group reported that PAR2 deficiency was associated with reduced atherosclerosis in the *apoE*$^{-/-}$ model.[43]

PAR2 deficiency was associated with reduced levels of pro-atherosclerotic chemokines in both the plasma and atherosclerotic lesions. We further demonstrated that treatment of VSMCs with various ligands leads to CCL2 and CXCL1 expression, secretion, and resultant monocyte chemotaxis, and that these responses were attenuated in PAR2 deficient cells. These results suggest that non-hematopoietic PAR2 contributes to the formation of atherosclerosis. This suggests that targeting PAR2 may reduce atherosclerosis and stabilize plaques.

Elevated levels of TF, and associated PAR2 activating proteases FVIIa and FXa, are observed in human atherosclerotic plaques and TF expression increases in conjunction with human atherosclerotic progression.[44–47] Importantly, TF is highly expressed in mouse models of atherosclerosis.[48, 49] However, heterozygous TF mice (*apoE*$^{-/-}$/*TF*$^{+/-}$) and a deficiency of TF in bone marrow cells (transplanted into an *Ldlr*$^{-/-}$ model) did not attenuate atherosclerosis versus control mice.[50] The contribution of non-hematopoietic cell TF could not be analyzed due to premature death in whole body TF deficient mice (apoE$^{-/-}$/low TF). However, similar to our study, Zhou and colleagues showed that FXa inhibition with rivaroxaban increased the thickness of protective fibrous caps and decreased aortic CCL2 in advanced lesions of *apoE*$^{-/-}$ mice compared to placebo controls.[51] Moreover, Hara and colleagues found that rivaroxaban administration to *apoE*$^{-/-}$ mice for 20 weeks reduced atherosclerotic burden in the aortic sinus and the aortic root.[16] Similar to our observations with PAR2 atherosclerotic lesions in PAR2 deficient mice, Hara and colleagues demonstrated rivaroxaban treatment resulted in significantly less lipid deposits, macrophage accumulation, more collagen deposition, and a trend toward increased SMC α-actin staining. Both of these publications with rivaroxaban hypothesized the actions of the drug occurred through inhibition of FXa signalling via either PAR2 and/or PAR1. Given the lack of protection with PAR1 deletion and the similarities between rivaroxaban and our data with

PAR2 deletion, we postulate that the protective actions of rivaroxaban on atherosclerosis may occur through inhibition of FXa-PAR2 signalling.

Atherosclerosis progression induces VSMC phenotypic switching toward a proinflammatory phenotype resulting in dedifferentiation and loss of medial SMC α-actin and other selective VSMC-defining contractile markers and subsequent migration into the lesion.[52] We observe that PAR2 deficiency attenuated the loss of medial VSMC α-actin in early lesions while increasing fibrous cap thickness and strength (Type I collagen) in advanced lesions. These results are also indicative of a vulnerable plaque phenotype characterized by the presence of large lipid-rich vacuoles covered by thin fibrous caps, decreased Type I collagen content, and the accumulation of macrophages[53]; which are all reversed with PAR2 deficiency. When combined with our studies demonstrating this effect is non-hematopoietic coupled with the role of PAR2 in VSMC mitogenesis, it is likely PAR2 is mediating atherosclerosis via a VSMC-mediated mechanism. We further speculate that VSMC PAR2 represents a primary source of CCL2, CXCL1, and resultant monocyte infiltration based on our chimeric and in vitro experiments. Paramount to this speculation is that PAR2 deficiency attenuates VSMC-induced monocyte chemotaxis via oxidized LDL and the CCL2 master-regulators IL-1β and TNFα.[40–42] Future studies will determine the effects of VSMC PAR2 using cell-specific deletions.

We have previously demonstrated that oxLDL can induce the expression of TF via activation of a TLR4 – TLR6 – CD36 heterotrimeric complex in hyperlipidemia resulting in the activation of coagulation.[54] Interestingly, we show that oxLDL stimulation of PAR2 deficient VSMCs express significantly less CCL2 and have reduced monocyte chemotaxis compared to proficient cells. Previous studies have shown that there is cross-talk between PAR2 and TLR4 where activation of PAR2 can enhance TLR4-dependent signaling.[55] Indeed, PAR2 interacts with TLR4 via cytoplasmic binding to myeloid differentiation factor 88 (MyD88) as well as MyD88-independent signaling via cytoplasmic binding to toll-like receptor adaptor molecule 1 (TRIF) during LPS-induced endotoxemia.[55] Furthermore, TLR4 deficient mice have reduced aortic PAR2 expression and decreased responsiveness to PAR2-AP in macrophages.[55, 56] In addition, oxLDL induction of CCL2 expression in VSMCs is reduced in TLR4 deficient cells, which is comparable to our results with PAR2.[57] Given these comparisons and the large literature on TLR4 and atherosclerosis, it is reasonable to speculate PAR2 and TLR4 may work cooperatively in the formation and progression of atherosclerosis.

Recent studies have demonstrated that PAR2 deficiency (mice) and PAR2 inhibition (rats) leads to reduced weight gain and insulin resistance on a 60% high fat diet and a metabolic syndrome high carbohydrate and fat diet, respectively.[31, 58] Our results confirm that PAR2 deficiency results in attenuated weight gain during 12 weeks of ‘Western’ diet feeding studies with a 42% high fat diet. We also demonstrate PAR2 deficiency attenuated fat accumulation and liver weight in our 12 week study, similar to Badeanlou and colleagues.[31] However, our results suggest that PAR2 expression in both hematopoietic and non-hematopoietic cells may contribute to weight gain, while previous studies suggest that only non-hematopoietic PAR2 is involved. Further, we did not detect any differences in glucose metabolism or insulin resistance after 12 weeks of diet. As a result, we did not examine

differences during the 24 week time point. The different results from these studies may be due to a variety of factors ranging from different strains of PAR2 deficient mice, variations in dietary fat, room temperatures, and gut microbes present in different mouse facilities. We further demonstrate that these changes in weight had no inadvertent effects on our atherosclerotic outcomes by utilizing a synthetic diet and demonstrating no change in atherosclerosis (despite changes in weight) between the $Par2^{+/+}$ recipient groups in our bone marrow transplantation study.

In summary, our study demonstrates that PAR2 but not PAR1 plays a role in atherosclerosis in the $Ldlr^{-/-}$ model. Further, atherosclerotic plaques formed in PAR2 deficient mice had a more stable morphology. Mechanistic studies suggest that PAR2 on VSMCs enhances the expression of CCL2, CXCL1, and monocyte recruitment. These findings suggest that PAR2 may be a novel therapeutic target to reduce atherosclerosis and stabilize plaques.

Supplementary Material

Refer to Web version on PubMed Central for supplementary material.

Acknowledgments

We thank the countless undergraduate students who have worked on this project throughout the years. Thanks to Elizabeth Tarling at UCLA for her invaluable feedback.

Sources of Funding

This work was supported by National Institutes of Health NHLBI grants 5R00-HL116786-05 (A.P.O. III), 5R01-HL132111-02 (M.T.).

Nonstandard Abbreviations and Acronyms

ApoE	Apolipoprotein E
DTI	Direct thrombin inhibitors
LDL	Low density lipoprotein
LPS	Lipopolysaccharide
MCP-1	Monocyte chemoattractant protein 1
MyD88	Myeloid differentiation factor 88
oxLDL	Oxidized low density lipoprotein
PAR	Protease activated receptor
TF	Tissue factor
TLR	Toll-like receptor
TRIF	Toll-like receptor adaptor molecule 1
VSMC	Vascular smooth muscle cell

References & Works Cited

1. Ross R. Atherosclerosis--an inflammatory disease. N Engl J Med. 1999; 340:115–126. [PubMed: 9887164]
2. Puente XS, Sanchez LM, Gutierrez-Fernandez A, Velasco G, Lopez-Otin C. A genomic view of the complexity of mammalian proteolytic systems. Biochem Soc Trans. 2005; 33:331–334. [PubMed: 15787599]
3. Coughlin SR. Thrombin signalling and protease-activated receptors. Nature. 2000; 407:258–264. [PubMed: 11001069]
4. Mann KG. Thrombin formation. Chest. 2003; 124:4S–10S. [PubMed: 12970118]
5. Borissoff JI, Otten JJ, Heeneman S, et al. Genetic and pharmacological modifications of thrombin formation in apolipoprotein e-deficient mice determine atherosclerosis severity and atherothrombosis onset in a neutrophil-dependent manner. PLoS One. 2013; 8:e55784. [PubMed: 23409043]
6. Bea F, Kreuzer J, Preusch M, Schaab S, Isermann B, Rosenfeld ME, Katus H, Blessing E. Melagatran reduces advanced atherosclerotic lesion size and may promote plaque stability in apolipoprotein e-deficient mice. Arterioscler Thromb Vasc Biol. 2006; 26:2787–2792. [PubMed: 16990551]
7. Vicente CP, He L, Tollefsen DM. Accelerated atherogenesis and neointima formation in heparin cofactor ii deficient mice. Blood. 2007; 110:4261–4267. [PubMed: 17878401]
8. Hamilton JR, Cornelissen I, Mountford JK, Coughlin SR. Atherosclerosis proceeds independently of thrombin-induced platelet activation in apoe−/− mice. Atherosclerosis. 2009; 205:427–432. [PubMed: 19217621]
9. Schini-Kerth VB, Bassus S, Fisslthaler B, Kirchmaier CM, Busse R. Aggregating human platelets stimulate the expression of thrombin receptors in cultured vascular smooth muscle cells via the release of transforming growth factor-beta1 and platelet-derived growth factorab. Circulation. 1997; 96:3888–3896. [PubMed: 9403612]
10. Papadaki M, Ruef J, Nguyen KT, Li F, Patterson C, Eskin SG, McIntire LV, Runge MS. Differential regulation of protease activated receptor-1 and tissue plasminogen activator expression by shear stress in vascular smooth muscle cells. Circ Res. 1998; 83:1027–1034. [PubMed: 9815150]
11. Nguyen KT, Frye SR, Eskin SG, Patterson C, Runge MS, McIntire LV. Cyclic strain increases protease-activated receptor-1 expression in vascular smooth muscle cells. Hypertension. 2001; 38:1038–1043. [PubMed: 11711494]
12. Borissoff JI, Spronk HM, Heeneman S, ten Cate H. Is thrombin a key player in the ‘coagulation-atherogenesis’ maze? Cardiovasc Res. 2009; 82:392–403. [PubMed: 19228706]
13. Lin H, Liu AP, Smith TH, Trejo J. Cofactoring and dimerization of proteinase-activated receptors. Pharmacol Rev. 2013; 65:1198–1213. [PubMed: 24064459]
14. Sevigny LM, Austin KM, Zhang P, Kasuda S, Koukos G, Sharifi S, Covic L, Kuliopulos A. Protease-activated receptor-2 modulates protease-activated receptor-1-driven neointimal hyperplasia. Arterioscler Thromb Vasc Biol. 2011; 31:e100–106. [PubMed: 21940952]
15. Marutsuka K, Hatakeyama K, Sato Y, Yamashita A, Sumiyoshi A, Asada Y. Protease-activated receptor 2 (par2) mediates vascular smooth muscle cell migration induced by tissue factor/factor viia complex. Thromb Res. 2002; 107:271–276. [PubMed: 12479889]
16. Hara T, Fukuda D, Tanaka K, Higashikuni Y, Hirata Y, Nishimoto S, Yagi S, Yamada H, Soeki T, Wakatsuki T, Shimabukuro M, Sata M. Rivaroxaban, a novel oral anticoagulant, attenuates atherosclerotic plaque progression and destabilization in apoe-deficient mice. Atherosclerosis. 2015; 242:639–646. [PubMed: 25817329]
17. Napoli C, de Nigris F, Wallace JL, Hollenberg MD, Tajana G, De Rosa G, Sica V, Cirino G. Evidence that protease activated receptor 2 expression is enhanced in human coronary atherosclerotic lesions. Journal of clinical pathology. 2004; 57:513–516. [PubMed: 15113859]
18. Demetz G, Seitz I, Stein A, Steppich B, Groha P, Brandl R, Schomig A, Ott I. Tissue factor-factor viia complex induces cytokine expression in coronary artery smooth muscle cells. Atherosclerosis. 2010; 212:466–471. [PubMed: 20708733]

19. Owens GK, Kumar MS, Wamhoff BR. Molecular regulation of vascular smooth muscle cell differentiation in development and disease. Physiol Rev. 2004; 84:767–801. [PubMed: 15269336]
20. Campbell JH, Campbell GR. The role of smooth muscle cells in atherosclerosis. Curr Opin Lipidol. 1994; 5:323–330. [PubMed: 7858906]
21. Worth NF, Rolfe BE, Song J, Campbell GR. Vascular smooth muscle cell phenotypic modulation in culture is associated with reorganisation of contractile and cytoskeletal proteins. Cell Motil Cytoskeleton. 2001; 49:130–145. [PubMed: 11668582]
22. Damiano BP, Cheung WM, Santulli RJ, Fung-Leung WP, Ngo K, Ye RD, Darrow AL, Derian CK, de Garavilla L, Andrade-Gordon P. Cardiovascular responses mediated by protease-activated receptor-2 (par-2) and thrombin receptor (par-1) are distinguished in mice deficient in par-2 or par-1. J Pharmacol Exp Ther. 1999; 288:671–678. [PubMed: 9918574]
23. Darrow AL, Fung-Leung WP, Ye RD, Santulli RJ, Cheung WM, Derian CK, Burns CL, Damiano BP, Zhou L, Keenan CM, Peterson PA, Andrade-Gordon P. Biological consequences of thrombin receptor deficiency in mice. Thromb Haemost. 1996; 76:860–866. [PubMed: 8972001]
24. Teupser D, Persky AD, Breslow JL. Induction of atherosclerosis by low-fat, semisynthetic diets in ldl receptor-deficient c57bl/6j and fvb/nj mice: Comparison of lesions of the aortic root, brachiocephalic artery, and whole aorta (en face measurement). Arterioscler Thromb Vasc Biol. 2003; 23:1907–1913. [PubMed: 12907460]
25. Daugherty A, Whitman SC. Quantification of atherosclerosis in mice. Methods Mol Biol. 2003; 209:293–309. [PubMed: 12357958]
26. Lu H, Rateri DL, Daugherty A. Immunostaining of mouse atherosclerotic lesions. Methods Mol Med. 2007; 139:77–94. [PubMed: 18287665]
27. Owens AP 3rd, Subramanian V, Moorleghen JJ, Guo Z, McNamara CA, Cassis LA, Daugherty A. Angiotensin ii induces a region-specific hyperplasia of the ascending aorta through regulation of inhibitor of differentiation 3. Circ Res. 2010; 106:611–619. [PubMed: 20019328]
28. Geisterfer AA, Peach MJ, Owens GK. Angiotensin ii induces hypertrophy, not hyperplasia, of cultured rat aortic smooth muscle cells. Circ Res. 1988; 62:749–756. [PubMed: 3280155]
29. Vrana M, Goodling A, Afkarian M, Prasad B. An optimized method for protein extraction from oct-embedded human kidney tissue for protein quantification by lc-ms/ms proteomics. Drug Metab Dispos. 2016; 44:1692–1696. [PubMed: 27481856]
30. Kagota S, Chia E, McGuire JJ. Preserved arterial vasodilatation via endothelial protease-activated receptor-2 in obese type 2 diabetic mice. Br J Pharmacol. 2011; 164:358–371. [PubMed: 21426317]
31. Badeanlou L, Furlan-Freguia C, Yang G, Ruf W, Samad F. Tissue factor-protease-activated receptor 2 signaling promotes diet-induced obesity and adipose inflammation. Nat Med. 2011; 17:1490–1497. [PubMed: 22019885]
32. Bennett MR, Sinha S, Owens GK. Vascular smooth muscle cells in atherosclerosis. Circ Res. 2016; 118:692–702. [PubMed: 26892967]
33. Berger P, Perng DW, Thabrew H, Compton SJ, Cairns JA, McEuen AR, Marthan R, Tunon De Lara JM, Walls AF. Tryptase and agonists of par-2 induce the proliferation of human airway smooth muscle cells. J Appl Physiol (1985). 2001; 91:1372–1379. [PubMed: 11509538]
34. Bono F, Lamarche I, Herbert JM. Induction of vascular smooth muscle cell growth by selective activation of the proteinase activated receptor-2 (par-2). Biochem Biophys Res Commun. 1997; 241:762–764. [PubMed: 9434782]
35. Bretschneider E, Kaufmann R, Braun M, Wittpoth M, Glusa E, Nowak G, Schror K. Evidence for proteinase-activated receptor-2 (par-2)-mediated mitogenesis in coronary artery smooth muscle cells. Br J Pharmacol. 1999; 126:1735–1740. [PubMed: 10372815]
36. Koo BH, Chung KH, Hwang KC, Kim DS. Factor xa induces mitogenesis of coronary artery smooth muscle cell via activation of par-2. FEBS Lett. 2002; 523:85–89. [PubMed: 12123809]
37. Wronkowitz N, Gorgens SW, Romacho T, Villalobos LA, Sanchez-Ferrer CF, Peiro C, Sell H, Eckel J. Soluble dpp4 induces inflammation and proliferation of human smooth muscle cells via protease-activated receptor 2. Biochim Biophys Acta. 2014; 1842:1613–1621. [PubMed: 24928308]

38. Hamilton JR, Frauman AG, Cocks TM. Increased expression of protease-activated receptor-2 (par2) and par4 in human coronary artery by inflammatory stimuli unveils endothelium-dependent relaxations to par2 and par4 agonists. Circ Res. 2001; 89:92–98. [PubMed: 11440983]

39. Radulovic M, Yoon H, Wu J, Mustafa K, Fehlings MG, Scarisbrick IA. Genetic targeting of protease activated receptor 2 reduces inflammatory astrogliosis and improves recovery of function after spinal cord injury. Neurobiol Dis. 2015; 83:75–89. [PubMed: 26316358]

40. Chen YM, Chiang WC, Lin SL, Wu KD, Tsai TJ, Hsieh BS. Dual regulation of tumor necrosis factor-alpha-induced ccl2/monocyte chemoattractant protein-1 expression in vascular smooth muscle cells by nuclear factor-kappab and activator protein-1: Modulation by type iii phosphodiesterase inhibition. J Pharmacol Exp Ther. 2004; 309:978–986. [PubMed: 14978197]

41. Parry GC, Martin T, Felts KA, Cobb RR. Il-1beta-induced monocyte chemoattractant protein-1 gene expression in endothelial cells is blocked by proteasome inhibitors. Arterioscler Thromb Vasc Biol. 1998; 18:934–940. [PubMed: 9633934]

42. Lim JH, Um HJ, Park JW, Lee IK, Kwon TK. Interleukin-1beta promotes the expression of monocyte chemoattractant protein-1 in human aorta smooth muscle cells via multiple signaling pathways. Exp Mol Med. 2009; 41:757–764. [PubMed: 19561397]

43. Zuo P, Zuo Z, Zheng Y, Wang X, Zhou Q, Chen L, Ma G. Protease-activated receptor-2 deficiency attenuates atherosclerotic lesion progression and instability in apolipoprotein e-deficient mice. Front Pharmacol. 2017; 8:647. [PubMed: 28959204]

44. Wilcox JN, Smith KM, Schwartz SM, Gordon D. Localization of tissue factor in the normal vessel wall and in the atherosclerotic plaque. Proc Natl Acad Sci U S A. 1989; 86:2839–2843. [PubMed: 2704749]

45. Thiruvikraman SV, Guha A, Roboz J, Taubman MB, Nemerson Y, Fallon JT. In situ localization of tissue factor in human atherosclerotic plaques by binding of digoxigenin-labeled factors viia and x. Lab Invest. 1996; 75:451–461. [PubMed: 8874378]

46. Marmur JD, Thiruvikraman SV, Fyfe BS, Guha A, Sharma SK, Ambrose JA, Fallon JT, Nemerson Y, Taubman MB. Identification of active tissue factor in human coronary atheroma. Circulation. 1996; 94:1226–1232. [PubMed: 8822973]

47. Hatakeyama K, Asada Y, Marutsuka K, Sato Y, Kamikubo Y, Sumiyoshi A. Localization and activity of tissue factor in human aortic atherosclerotic lesions. Atherosclerosis. 1997; 133:213–219. [PubMed: 9298681]

48. Bea F, Blessing E, Shelley MI, Shultz JM, Rosenfeld ME. Simvastatin inhibits expression of tissue factor in advanced atherosclerotic lesions of apolipoprotein e deficient mice independently of lipid lowering: Potential role of simvastatin-mediated inhibition of egr-1 expression and activation. Atherosclerosis. 2003; 167:187–194. [PubMed: 12818400]

49. Monetti M, Canavesi M, Camera M, Parente R, Paoletti R, Tremoli E, Corsini A, Bellosta S. Rosuvastatin displays anti-atherothrombotic and anti-inflammatory properties in apoe-deficient mice. Pharmacol Res. 2007; 55:441–449. [PubMed: 17350858]

50. Tilley RE, Pedersen B, Pawlinski R, Sato Y, Erlich JH, Shen Y, Day S, Huang Y, Eitzman DT, Boisvert WA, Curtiss LK, Fay WP, Mackman N. Atherosclerosis in mice is not affected by a reduction in tissue factor expression. Arterioscler Thromb Vasc Biol. 2006; 26:555–562. [PubMed: 16385085]

51. Zhou Q, Bea F, Preusch M, Wang H, Isermann B, Shahzad K, Katus HA, Blessing E. Evaluation of plaque stability of advanced atherosclerotic lesions in apo e-deficient mice after treatment with the oral factor xa inhibitor rivaroxaban. Mediators Inflamm. 2011; 2011:432080. [PubMed: 21772662]

52. Chistiakov DA, Orekhov AN, Bobryshev YV. Vascular smooth muscle cell in atherosclerosis. Acta Physiol (Oxf). 2015; 214:33–50. [PubMed: 25677529]

53. Naghavi M, Libby P, Falk E, et al. From vulnerable plaque to vulnerable patient: A call for new definitions and risk assessment strategies: Part i. Circulation. 2003; 108:1664–1672. [PubMed: 14530185]

54. Owens AP 3rd, Passam FH, Antoniak S, et al. Monocyte tissue factor-dependent activation of coagulation in hypercholesterolemic mice and monkeys is inhibited by simvastatin. J Clin Invest. 2012

55. Rallabhandi P, Nhu QM, Toshchakov VY, Piao W, Medvedev AE, Hollenberg MD, Fasano A, Vogel SN. Analysis of proteinase-activated receptor 2 and tlr4 signal transduction: A novel paradigm for receptor cooperativity. J Biol Chem. 2008; 283:24314–24325. [PubMed: 18622013]

56. Bucci M, Vellecco V, Harrington L, Brancaleone V, Roviezzo F, Mattace Raso G, Ianaro A, Lungarella G, De Palma R, Meli R, Cirino G. Cross-talk between toll-like receptor 4 (tlr4) and proteinase-activated receptor 2 (par(2)) is involved in vascular function. Br J Pharmacol. 2013; 168:411–420. [PubMed: 22957757]

57. Guo L, Chen CH, Zhang LL, et al. Irak1 mediates tlr4-induced abca1 downregulation and lipid accumulation in vsmcs. Cell Death Dis. 2015; 6:e1949. [PubMed: 26512959]

58. Lim J, Iyer A, Liu L, Suen JY, Lohman RJ, Seow V, Yau MK, Brown L, Fairlie DP. Diet-induced obesity, adipose inflammation, and metabolic dysfunction correlating with par2 expression are attenuated by par2 antagonism. FASEB J. 2013; 27:4757–4767. [PubMed: 23964081]

Highlights

1. Deficiency of protease-activated receptor 2 attenuates the development of acute and chronic atherosclerosis.
2. PAR2 deficiency confers a protective plaque phenotype
3. PAR2 deficiency in non-hematopoietic cells is atheroprotective
4. PAR2 regulates the production of MCP-1 and promotes monocyte chemotaxis

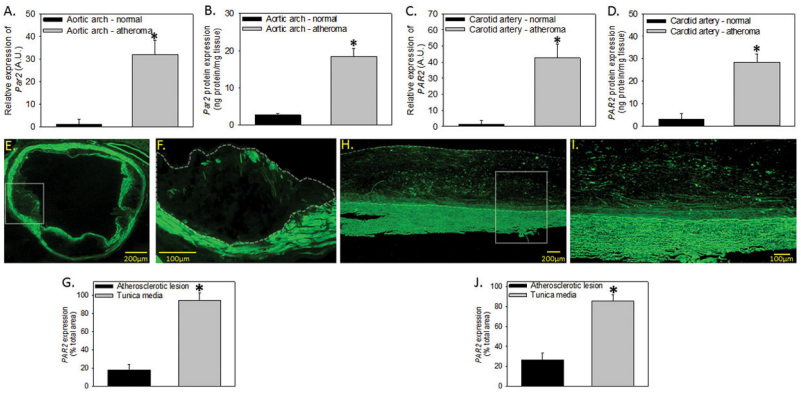

Figure 1. PAR2 mRNA and protein are increased in the atherosclerotic prone regions of mice and humans

Normal mouse aortic arch (*Ldlr*$^{-/-}$ mice fed a chow ® diet for 24 weeks) or atherosclerosis-containing aortic arches (*Ldlr*$^{-/-}$ mice fed a 'Western' diet for 24 weeks) were examined for (A) mRNA extrapolated to normal and (B) protein expression (n = 5 individual samples/group). Normal or diseased human carotid arteries were isolated and examined for (C) mRNA extrapolated to normal and (D) protein expression (n = 5 individual samples/group). Immunologic detection of PAR2 expression was also performed on mouse atherosclerotic aortic sinus (E – F) and human carotid atherosclerotic lesions (H – I; n = 4 – 5 individual samples/species; 4 x mag E & H; 10 x mag F & I). (G & J) Quantification of PAR2 staining in the lesion or media of atherosclerotic lesions. Solid white box is zoomed in area. Dashed white line is the area of the lesion. Histobars represent mean ± SEM. * Denotes $P < 0.05$ for comparisons to normal aorta/artery or lesion versus tunica media (Two-tailed Student's t-test).

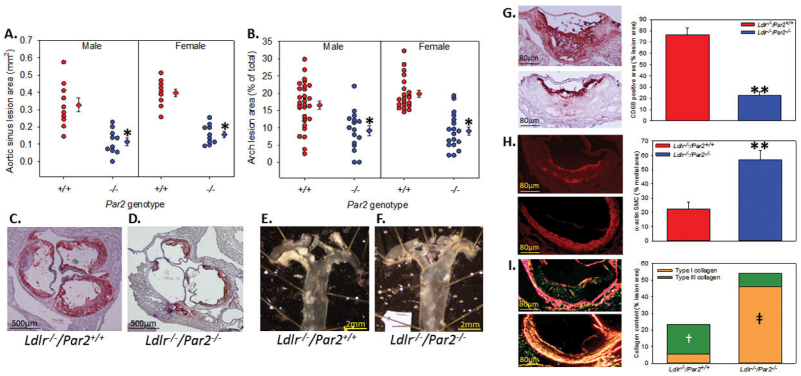

Figure 2. PAR2 deficiency reduces the formation of early atherosclerosis

Male and female *Ldlr*$^{-/-}$ mice that were *Par2*$^{+/+}$ and −/− (n = 16 – 30) were fed a high fat/cholesterol diet for 12 weeks. (A) Percent lesion area of the aortic sinus and (B) en face area of the aortic arch where circles represent individual measurements, diamonds are means ± SEM. * Denotes P = 0.001 for comparisons of −/− to +/+ (Two-way ANOVA with Holm-sidak post hoc). (C,D) Representative images of Oil-red O stained aortic sinus and (E,F) unstained en face images of the aortic arch. Representative images and quantification of (G) CD68, (H) SMC α-actin, and (I) picrosirius red stained aortic sinus lesions (*Ldlr*$^{-/-}$/*Par2*$^{+/+}$ - top; *Ldlr*$^{-/-}$/*Par2*$^{-/-}$ - bottom). Histobars represent means ± SEM. ** Denotes P < 0.005 for comparison of −/− to +/+ (two-tailed Student's t-test). ǂ Denotes P < 0.001 for comparison of −/− to +/+ and † denotes P < 0.05 for comparison of +/+ to −/− (One way ANOVA on Ranks with Dunn's post hoc).

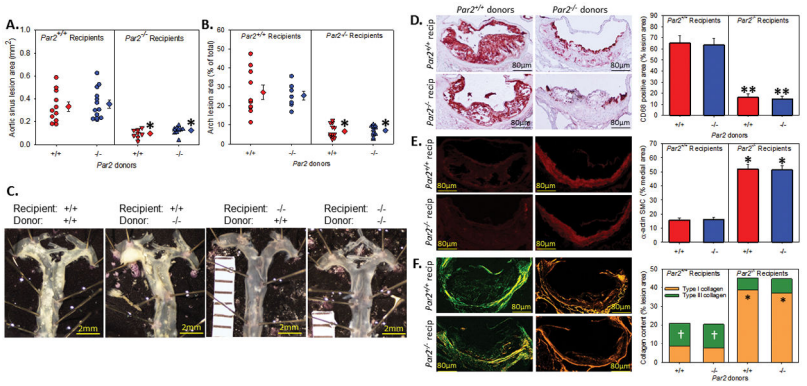

Figure 3. Non-hematopoietic PAR2 reduces atherosclerosis

Male *Ldlr*$^{-/-}$/*Par2*$^{+/+}$ and *Ldlr*$^{-/-}$/*Par2*$^{-/-}$ mice (8–10 weeks old, n = 10 – 12 each group) were irradiated (1300 rads split into two equal doses four hours apart) and repopulated with *Par2*$^{+/+}$ or $^{-/-}$ bone marrow. Mice were allowed to recover for 5 weeks, and then fed a Western diet for 12 weeks. (A) Percent lesion area of the aortic sinus and (B) en face area of the aortic arch where circles represent individual measurements, diamonds are means ± SEM. (C) Representative images of unstained en face images of the aortic arch. Representative images and quantification of (D) CD68, (E) SMC α-actin, and (F) picrosirius red stained aortic sinus lesions. Histobars represent means ± SEM. * Denotes P = 0.001, ** denotes P < 0.05 for comparisons of −/− to +/+; † denotes P < 0.05 for comparison of +/+ to −/− (A, B, D: Two-way ANOVA with Holm-sidak post hoc; C, E: Two-way ANOVA on Ranks Dunn's post hoc).

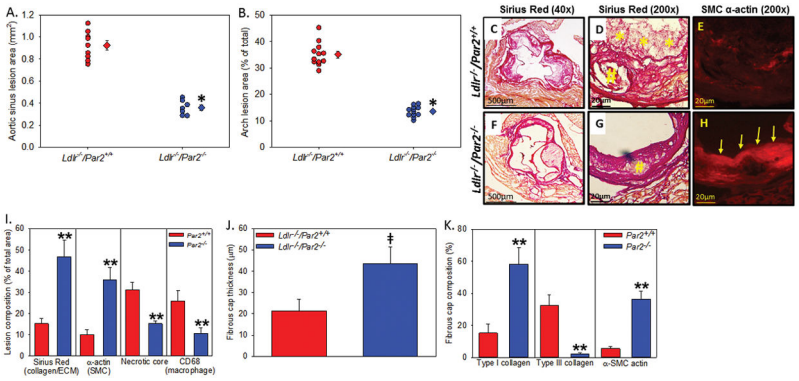

Figure 4. PAR2 deficiency attenuates the formation of advanced atherosclerosis and increases plaque stability

Male *Ldlr*$^{-/-}$ mice (8–12 weeks) that were *Par2*$^{+/+}$ and −/− (n = 12) were fed a high fat/cholesterol diet for 24 weeks. (A) Percent lesion area of the aortic sinus and (B) en face area of the aortic arch where circles represent individual measurements, diamonds are means ± SEM. (C–D and F–G) Sirius red stain for collagen at 40x magnification (C,D) and 200x magnification (D,G). Yellow * and # represent secondary atherosclerotic lesions and necrotic core, respectively. (E,H) SMC α-actin immunofluorescence where yellow arrows highlight the SMC cap in the −/− mice. Quantification of (I) aortic sinus lesion collagen, SMC, necrotic core, and CD68; (J) fibrous cap thickness; and (K) fibrous cap composition of collagen and SMC α-actin). Histobars represent means ± SEM. * Denotes P = 0.001 (Mann-Whitney Rank Sum), ‡ denotes P < 0.05 (Mann Whitney U test), ** P < 0.05 (ANOVA on ranks Dunn's post hoc) for comparisons of −/− to +/+.

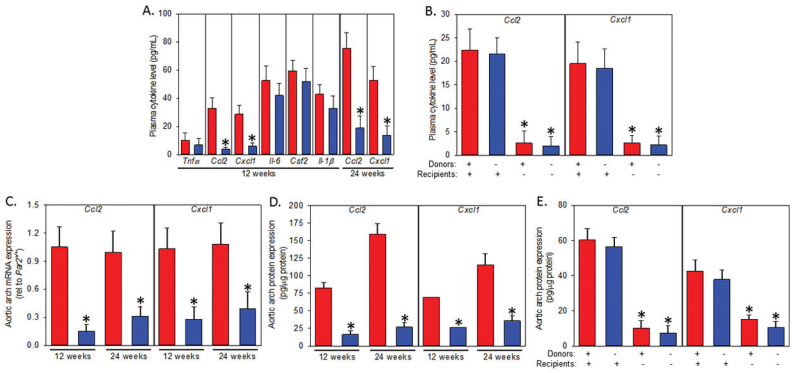

Figure 5. PAR2 deficiency attenuates *CCL2* and C*xcl1* in the plasma and atherosclerotic lesions

Plasma cytokines were analyzed from aforementioned (A) 12 and 24 week 'Western' diet fed $Ldlr^{-/-}/Par2^{+/+}$ and $Ldlr^{-/-}/Par2^{-/-}$ mice and (B) $Ldlr^{-/-}/Par2^{+/+}$ and $Ldlr^{-/-}/Par2^{-/-}$ irradiated and repopulated ($Par2^{+/+}$ or $^{-/-}$ bone marrow) mice. Additionally $Ldlr^{-/-}/Par2^{+/+}$ and $Ldlr^{-/-}/Par2^{-/-}$ mice, and a cohort of similarly irradiated and repopulated mice, were fed a 'Western' diet for 12 (normal and irradiated) and 24 weeks (normal) and their aortic arches (from aortic sinus to end of the subclavian artery) were harvested and processed for (C) mRNA and (D – E) protein examining the chemokines *Ccl2* and *Cxcl1* (n = 5 each time point and genotype). Histobars represent means ± SEM. * Denotes $P < 0.01$ for comparisons of −/− to +/+ and −/− recipients to +/+ recipients (ANOVA on ranks with Dunn's post hoc analysis). Red histobars represent $Ldlr^{-/-}/Par2^{+/+}$ (and +/+ donors) and blue histobars represent $Ldlr^{-/-}/Par2^{-/-}$ (and −/− donors) mice.

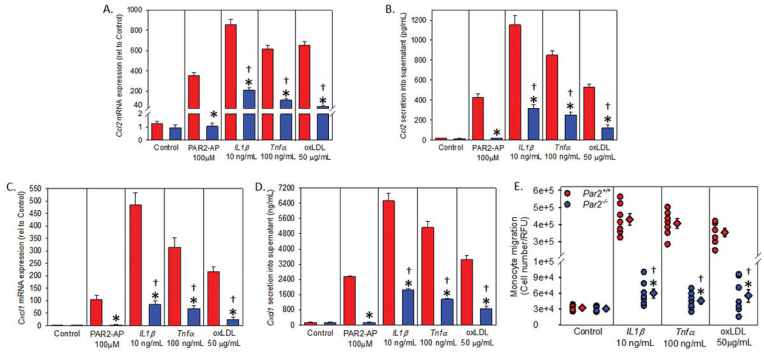

Figure 6. *Ccl2* and *Cxcl1* expression and secretion is reduced in PAR2 deficient VSMCs

Mouse aortic arch VSMCs were treated for (A & C) 4 or (B & D) 24 hrs with PAR2-AP (100 μM), *IL-1β* (10 ng/mL), *Tnfα* (100 ng/mL), or the atherogenic ligand oxidized LDL (oxLDL, 50 μg/mL) and mRNA extracted or protein supernatant quantified at respective time points. mRNA was extrapolated to placebo control (LDL, 50 μg/mL). (E) $Par2^{+/+}$ and $Par2^{-/-}$ mouse VSMCs were treated with placebo control (LDL, 50 μg/mL), *IL-1β* (10 ng/mL), *Tnfα* (100 ng/mL), or oxLDL (50 μg/mL) for 24 hours and monocytes were added to a transwell boyden chamber and infiltration/adhesion quantified (n = 6 performed in triplicate). Circles represent individual measurements, diamonds are means ± SEM. * $P < 0.001$ for comparisons of −/− to +/+ treatment groups; †$P < 0.05$ −/− treatment versus control (Two way ANOVA Tukey's post hoc). Red histobars represent $Ldlr^{-/-}/Par2^{+/+}$ and blue histobars represent $Ldlr^{-/-}/Par2^{-/-}$ mice.

Table 1

Metabolic and lipid parameters from study mice

Mouse group	Gender	Mouse number	Diet (weeks)	Weight (grams)	TPC (mg/dL)	HDL (mg/dL)	Trigs (mg/dL)
Ldlr$^{-/-}$/*Par2*$^{+/+}$	Female	21	12	37.8 ± 1.4*	1138 ± 73.1	201 ± 21.8	349 ± 42.8
Ldlr$^{-/-}$/*Par2*$^{-/-}$	Female	18	12	34.2 ± 0.9	1122 ± 52.8	191 ± 12.8	336 ± 23.4
Ldlr$^{-/-}$/*Par2*$^{+/+}$	Male	30	12	41.9 ± 1.2*	1173 ± 64.4	194 ± 26.9	394 ± 53.4
Ldlr$^{-/-}$/*Par2*$^{-/-}$	Male	16	12	37.3 ± 1.3	1097 ± 99.1	205 ± 59.7	364 ± 94.1
Ldlr$^{-/-}$/*Par2*$^{+/+}$	Male	12	24	43.2 ± 1.1	1187 ± 60.7	266 ± 13.9	719 ± 68.3
Ldlr$^{-/-}$/*Par2*$^{-/-}$	Male	12	24	41.3 ± 1.1	1165 ± 215.4	214 ± 37.9	647 ± 40.3
Ldlr$^{-/-}$/*Par2*$^{+/+}$ LFD	Male	9	12	26.5 ± 1.3	1098 ± 42.8	205 ± 25.8	318 ± 41.9
Ldlr$^{-/-}$/*Par2*$^{-/-}$ LFD	Male	9	12	26.7 ± 1.2	1125 ± 39.6	219 ± 41.8	357 ± 42.8
Ldlr$^{-/-}$/*Par1*$^{+/+}$	Male	15	12	42.1 ± 1.7	1204 ± 72.8	192 ± 26.8	419 ± 38.4
Ldlr$^{-/-}$/*Par1*$^{-/-}$	Male	16	12	41.7 ± 1.4	1249 ± 64.7	211 ± 18.9	448 ± 53.7
Par2$^{+/+}$ into *Par2*$^{+/+}$	Male	11	12	36.0 ± 1.5†	1221 ± 48.3	168 ± 24.5	293 ± 43.7
Par2$^{-/-}$ into *Par2*$^{+/+}$	Male	13	12	32.5 ± 0.8	1131 ± 52.9	173 ± 21.1	250 ± 17.4
Par2$^{+/+}$ into *Par2*$^{-/-}$	Male	13	12	31.8 ± 1.1	1076 ± 65.2	154 ± 14.9	285 ± 39.0
Par2$^{-/-}$ into *Par2*$^{-/-}$	Male	12	12	30.8 ± 1.1	1124 ± 51.4	159 ± 31.2	300 ± 15.5

Abbreviations: LFD – low fat diet; TPC – total plasma cholesterol; HDL – high density lipoprotein; Trigs – Triglycerides. All mice were fed a 'Western' diet, except the LFD group, which was fed a semi-synthetic diet.

All weights are taken at the end of the study and plasma parameters measured from terminal blood collection.

*P < 0.01 versus Par2−/− mice; Mann Whitney Rank U.

†P < 0.008 versus all other chimeric groups; ANOVA on Ranks.